INSTITUTE OF PHYSICS PUBLISHING JOURNAL OF PHYSICS B: ATOMIC, MOLECULAR AND OPTICAL PHYSICS

J. Phys. B: At. Mol. Opt. Phys. **35** (2002) 605–626 PII: S0953-4075(02)24907-X

On the use of classical transport analysis to determine cross-sections for low-energy e–H_2 vibrational excitation

R D White[1,2], **Michael A Morrison**[1] **and B A Mason**[1]

[1] Department of Physics & Astronomy, University of Oklahoma, Norman, OK 73019, USA
[2] School of Mathematical and Physical Sciences, James Cook University, Cairns, QLD 4870, Australia

Received 11 May 2001, in final form 12 December 2001
Published 31 January 2002
Online at stacks.iop.org/JPhysB/35/605

Abstract

The long-standing discrepancy between the theoretically and experimentally determined $v = 0 \rightarrow 1$ vibrational cross-section of hydrogen is addressed by analysing the transport theory used to deconvolute electron swarm transport data. The implementation of the full energy and angular dependence of quantum mechanically derived differential cross-sections in the semiclassical transport theory (using both a multi-term Boltzmann equation solution and an independent Monte Carlo simulation) is shown to be unable to resolve the discrepancy. Assumptions and approximations used in the original transport analyses are quantified and validated.

1. Introduction

For over 30 years, the field of electron–molecule scattering has been plagued by a severe discrepancy between vibrational cross-sections obtained using beam and swarm measurements. This discrepancy first appeared in the late 1960s and early 1970s, when crossed-beam data from measurements by Ehrhardt *et al* (1968) of integral cross-sections for the electron-induced $v_0 = 0 \rightarrow v = 1$ excitation of H_2 were compared with contemporaneous cross-sections determined by Crompton *et al* (see e.g. Huxley and Crompton 1974) from data taken in swarm experiments. Over the energy range from threshold to about 1.5 eV, the highest energy at which swarm-derived cross-sections could be determined with confidence, the two sets of data disagreed by as much as 60%—an amount greatly in excess of the errors and uncertainties claimed for each determination. Although a subsequent beam measurement by Linder and Schmidt (1971) confirmed the results of Ehrhardt *et al* (1968), the significance of the disparity with swarm-derived cross-sections was mitigated somewhat by the nature of these early beam experiments, which were designed to explore resonance effects in vibrational and electronic excitation rather than to measure absolute non-resonant cross-sections.

0953-4075/02/030605+22$30.00

To appreciate the nature of this discrepancy, it is important to understand that swarm experiments differ significantly from crossed-beam methodologies in that they do not yield cross-sections directly. Rather, a swarm experiment entails measuring physical properties of an electron swarm that is in a quasi-steady state determined by a balance between power input from an applied electric field $\boldsymbol{E}$ and energy loss rate via collisions between electrons in the swarm and particles of a neutral gas of density N. A set of cross-sections (which for low values of E/N includes the momentum transfer cross-section, rotational cross-sections and vibrational cross-section for all energetically allowed excitations) is determined that is consistent with the experimental raw data as follows.

The first step involves the experimental measurement of transport coefficients from swarm experiments (e.g. the drift velocity W, transverse and longitudinal diffusion coefficients D_{T} and D_{L} respectively and the rate coefficient k_i for the ith collision process) for a range of applied reduced fields E/N (see e.g. Huxley and Crompton 1974 for details).

The second step in the process involves the 'inversion' of the experimentally measured transport coefficients to obtain the interaction cross-sections. The equation which links the experimentally measured transport coefficients with the *unknown* interaction cross-sections is Boltzmann's equation. For a given set of cross-sections, all measurable quantities can be calculated from the solution of Boltzmann's equation. Rather than a direct inversion of Boltzmann's equation to determine the unknown interaction cross-sections, an iterative scheme is employed: an initial set of trial cross-sections is input into the Boltzmann equation and transport coefficients are theoretically determined over the range of E/N considered in the experimental measurements. The experimentally measured transport coefficients are then compared with the theoretically calculated transport coefficients for all values of E/N at which data were taken. The initial trial cross-section set is then iteratively adjusted and theoretical transport coefficients recalculated until a set of cross-sections is obtained from which the calculated transport coefficients match the experimentally measured transport coefficients (to within experimental error) over the entire range of E/N. This is then the set of cross-sections determined from swarm experiments. This was the procedure used by Crompton *et al* (1969, 1970) to generate the e–H_2 vibrational cross-sections which differed so strikingly from the crossed-beam results of Ehrhardt *et al* (1968) and Linder and Schmidt (1971).

Extensive research on e–H_2 vibrational excitation during the past two decades by theorists and experimentalists—as detailed in section 2—left the conundrum of vibrational excitation of H_2 at an impasse. The situation is quite serious, for more is at stake than low-energy vibrational cross-sections for this particular system. *For scattering energies from threshold to a few eV, swarm experiments remain the primary experimental source of inelastic and momentum-transfer cross-sections*. In addition to their fundamental importance, such cross-sections are in high demand for such diverse scientific and technological applications as astrophysics, lasers, energy-related technology and pollution control. If, indeed, prior determinations of vibrational cross-sections for e–H_2 and other systems by conventional transport analysis have been in error—one possible explanation for the disagreement of swarm-derived cross-sections with theoretical and beam-determined data—then analyses that rely on these cross-sections, such as laser kinetic modelling, may also be in error[3].

This paper reports the first phase of a new project to tackle this long-standing and exasperating problem from a completely different point of view, shifting attention to the transport theory itself. Our long-term goal, in brief, is to investigate key assumptions underlying existing analyses of swarm data. This project, a collaboration between OU and

[3] A similar disparity exists between theoretical and swarm-derived vibrational cross-sections for e–N_2 scattering (Sun *et al* 1995). But neither approach has been studied as extensively for the e–N_2 system as both have for e–H_2 (see section 2).

James Cook University, will combine a variety of approaches to the Boltzmann equation with Monte Carlo calculations which apply a microscopic semiclassical transport theory to the swarm experiments.

This first paper details tests of the suitability of the traditional semiclassical Boltzmann analysis under the conditions of the scattering process under question. Unlike, say, elastic electron–atom scattering, where agreement between swarm-derived and theoretical or other experimental cross-sections is excellent, or electron–molecule scattering under conditions such that only rotational excitation is involved, the problem at hand features electrons that lose energy to two scattering processes with distinctly different thresholds and energy losses: the threshold for the $j_0 = 0 \rightarrow j = 2$ rotational threshold is 0.044 eV, while that for the $v_0 = 0 \rightarrow v = 1$ vibrational excitation is 0.52 eV, more than an order of magnitude larger. Here, we present in section 4.2 foundation studies which compare results from semiclassical Boltzmann analysis and Monte Carlo simulations for collisions that satisfy these characteristics. These comparisons build on earlier studies by Reid (1979), as will be discussed in this section.

Section 2 summarizes prior attempts to resolve the disparity in e–H_2 vibrational cross-sections. Then in section 3, we review the fundamental equation used in the analysis of all swarm experiments—the semiclassical Boltzmann equation. In traditional analyses of swarm experiments (hereafter referred to as 'conventional theories') (Gibson 1970, Huxley and Crompton 1974), various approximations were implemented in the solution of this equation. These approximations are highlighted in section 3 along with the details of the present theory, which avoids them. In section 4.3, we present for the first time results using the full set of quantum mechanically derived anisotropic cross-sections of Morrison and Trail (1993), with no approximations in both the Boltzmann equation and Monte Carlo treatments. We focus exclusively on the simplest collision conditions for which swarm experiments have been performed: a swarm of electrons drifting and diffusing through pure *para*-hydrogen at a gas temperature of 77 K. We then turn our investigations to issues pertinent to approximations used in conventional theories used in the analysis of swarm experiments. The errors associated with certain of these approximations are quantified in section 4.4. Finally, section 4.5 contains a systematic investigation of the importance of anisotropic scattering for this system. Our conclusions, summarized in section 5, lay the foundation for the broader inquiries described above.

2. Background

Hydrogen is the simplest neutral molecular target, with many characteristics that make it ideal for experimental and theoretical study. It is non-polar. It has only two electrons. Its nuclei are light enough to justify a non-relativistic treatment. Its electronically excited and dissociative states are well separated in energy from low-lying rotational and vibrational levels of the ground electronic state. And in that state, the rotational and vibrational degrees of freedom are effectively uncoupled. So, in 1980, theorists at the University of Oklahoma (OU) and swarm experimentalists at the Australian National University (ANU) undertook a joint inquiry into low-energy electron–H_2 scattering. The goal was to attain a confirmation of electron–molecule collision physics comparable to that obtained in 1979 for electron–atom scattering, when Nesbet (1979) reported calculated *ab initio* theoretical low-energy e–He cross-sections that agreed with swarm-derived values at energies below the first electronically inelastic threshold to within 1%.

Much to the consternation of all concerned, this goal proved unattainable. While results from theoretical calculations and swarm experiments for the momentum transfer and rotational excitation agreed superbly, the vibrational excitation cross sections disagreed by as much as 60%—many times the most pessimistic error estimates for either study.

There followed many years of work by theorists at OU, the Joint Institute for Laboratory Astrophysics and the Lawrence Livermore Laboratory and by experimentalists at the ANU—all of whom sought to resolve the situation. At OU, theoretical efforts involved successive improvements in the rigour of the formulation, by eliminating approximations from the e–H_2 interaction potential and refining the representation of the rotational and vibrational dynamics in the solution of the Schrödinger equation. At the ANU, new transport analyses were undertaken, both of the original swarm data and of new data taken in mixture measurements, in which the electron swarm encounters a high concentration of a rare gas, whose momentum transfer cross-section is well known, and a small concentration of molecular hydrogen.

All this work, the details of which have been summarized in two interim reports (Morrison *et al* 1987, Crompton and Morrison 1993), left the situation virtually unchanged. The new analyses of swarm data for mixtures of H_2 and various rare gases yielded cross-sections in agreement with those obtained in a re-analysis of earlier transport coefficients for pure H_2 (England *et al* 1988). Yet, the most rigorous OU theoretical vibrational cross-sections remain persistently incompatible with the swarm-derived cross-sections. When inserted into the transport analysis, the theoretical cross sections yield transport coefficients that disagree with measured data by several per cent (Crompton and Morrison 1993), well outside the better-than-1% accuracy of those data. In their final report on the situation, Crompton and Morrison (1993) concluded 'We are . . . left with the possibility of an error or inconsistency in the analysis of swarm data in *molecular* gases, noting, however, that no such problems appear in the analysis for *atomic* gases. This possibility must be considered along with the other possible explanations of the persistent discrepancy (in the $0 \rightarrow 1$ vibrational cross-section), no matter how remote they may seem'.

Two additional recent pieces of research provide essential background and motivation for the present project: a new crossed-beam measurement of e–H_2 vibrational cross-sections, and a theoretical sensitivity study to the sole significant approximation remaining in the OU theoretical calculations.

In 1990, Buckman *et al* reported state-of-the-art crossed-beam measurements using a new apparatus designed to yield absolute low-energy cross-sections. The overall 90 meV energy resolution of this apparatus enabled direct comparison of the resulting vibrational cross-sections with swarm-derived values at energies as low as 1.0 eV, nearly twice the 0.52 eV threshold of the $0 \rightarrow 1$ excitation. In the important energy range below 1.5 eV, the new crossed-beam cross-sections agree within experimental error with the latest OU theoretical values and with the previous crossed-beam data of Ehrhardt *et al* (1968) and Linder and Schmidt (1971). But all these data are strikingly at odds with the swarm-derived cross-sections. Buckman *et al* (1990) remarked that they 'consider the present study to have settled [the] long-standing controversy [over the $0 \rightarrow 1$ e–H_2 cross-section]. In particular, the present [OU] theoretical formulation . . . appears to accurately describe the $0 \rightarrow 1$ excitation at these energies'. In conclusion, these authors call for 'a new investigation of electron transport in H_2 by Monte Carlo methods'.

The second recent piece of relevant research was a sensitivity study by Morrison and Trail (1993) of the e–H_2 interaction potential used in the OU theoretical calculations. In its most rigorous form, these calculations use converged close-coupling theory for the vibrational dynamics and an adiabatic treatment of rotation that had been shown previously to be highly accurate for energies at and above the first vibrational threshold. Furthermore, these calculations treat rigorously the non-local exchange interaction that arises from the anti-symmetrization postulate, using the same near-Hartree–Fock electronic H_2 wavefunction as in the static (Coulomb) interaction. Finally, they include a correlation-polarization potential that correctly includes adiabatically induced distortions of the target for projectile coordinates

outside the molecular charge cloud and that asymptotically yields polarizabilities in good agreement with measured values. The sole significant approximation in this formulation is the use of a 'non-penetrating approximation' to mimic the short-range, non-local, many-body effects of bound–free correlation, effects which come into play for projectile coordinates very near or within the molecular charge cloud.

Could errors in this approximate bound–free correlation potential be responsible for the disparity between theoretical and swarm-derived $0 \rightarrow 1$ cross-sections? Morrison and Trail (1993) addressed this question via a quantitative investigation of the sensitivity of all relevant e–H_2 cross sections—the momentum transfer, rotational excitation, integral elastic and differential elastic—to physically reasonable variations in the model correlation potential. In effect, the agreement of all these cross-sections with various experimental results (including swarm-derived values) place 'boundary conditions' on any mechanism—theoretical or otherwise—to explain the disparity in the vibrational cross-sections. In their study, Morrison and Trail (1993) found that any reasonable alteration to their bound–free correlation potential that yielded vibrational cross-sections consistent with the swarm-derived values seriously compromised the rotational and/or momentum transfer cross-sections.

3. Semiclassical Boltzmann theory

The governing equation for a swarm of electrons moving through a background gas of neutral molecules under the influence of a spatially homogeneous electric field ($\boldsymbol{E}$) is Boltzmann's equation for the phase space electron distribution function $f(\boldsymbol{r}, \boldsymbol{c}, t)$:

$$\frac{\partial f}{\partial t} + \boldsymbol{c} \cdot \nabla f - \frac{e\boldsymbol{E}}{m} \cdot \frac{\partial f}{\partial \boldsymbol{c}} = -\hat{J}(f), \tag{1}$$

where $\boldsymbol{r}$ and $\boldsymbol{c}$ denote respectively the position and velocity coordinates of an electron in the swarm, $\hat{J}(f)$ is the collision operator and t is the time. The electron mass and charge magnitude are m and e respectively. In all prior applications of Boltzmann theory to swarm experiments, the electron number density $n(\boldsymbol{r}, t)$ has been assumed to be sufficiently low that the following conditions pertain:

(1) electron–electron scattering can be neglected;
(2) the fermionic character of the electrons can be ignored, i.e. one need not take account of the Pauli exclusion principle in the collision integrals;
(3) the translational motion of the electrons can be treated classically;
(4) the background of neutral molecules remains in thermal equilibrium.

In swarm experiments the current is varied over several orders of magnitude to check for these effects. No changes in the experimentally measured quantities are observed, which indicates that space charge and the deviation of the neutral distributions from equilibrium may be negligible. The collision operator $\hat{J}(f)$ on the right-hand side of equation (1) thus represents only electron–neutral molecule interactions. In the present work we employ the original Boltzmann collision operator for elastic processes (Boltzmann 1872) and its semiclassical generalization for inelastic processes (Wang-Chang *et al* 1964):

$$\hat{J}(f) = \sum_{i,k} \int\int \left[f(\boldsymbol{r}, \boldsymbol{c}, t)\boldsymbol{F}_i(\boldsymbol{C}) - f(\boldsymbol{r}, \boldsymbol{c}', t)\boldsymbol{F}_k(\boldsymbol{C}') \right] v\sigma^{(i\rightarrow k)}(v, \theta) \sin\theta \, \mathrm{d}\theta \, \mathrm{d}\psi \, \mathrm{d}\boldsymbol{C}, \tag{2}$$

where $\boldsymbol{F}_k(\boldsymbol{C})$ denotes the velocity distribution of neutral molecules in the ro-vibrational state characterized by the index $k \equiv (v, j, m_j)$, and $\boldsymbol{C}$ is the velocity of the neutral molecule. Primes denote post-collision quantities. The differential cross-section for an electron that scatters into centre-of-mass angles θ and ψ and induces a transition in the neutral molecule from state i to

state k is $\sigma^{(i\to k)}(v,\theta)$, where v is the initial relative velocity of the electron and the molecule. We shall discuss further the role of the angular dependence of the differential cross-section in section 4. Here it suffices to say that the naturally occurring quantities in conventional Boltzmann theory are the Legendre projections of the differential cross-sections. These follow from the expansion

$$\sigma^{(i\to k)}(v,\theta) = \sum_{L=0}^{L_{\max}} \left(\frac{2L+1}{4\pi}\right) \sigma_L^{(i\to k)}(v) P_L(\cos\theta), \tag{3a}$$

and the orthogonality relation for Legendre polynomials as

$$\sigma_L^{(i\to k)}(v) = 2\pi \int_{-1}^{1} \sigma^{(i\to k)}(v,\theta) P_L(\cos\theta)\, \mathrm{d}(\cos\theta). \tag{3b}$$

Strictly speaking, the sum over L in (3a) includes an infinite number of terms, though in practice the modest angular variation of the differential cross-sections allows it to be truncated to high accuracy at only a few terms. We shall refer to the projections defined in equation (3b) as *partial differential cross-sections*.

Equations (1) and (2) constitute the semiclassical Boltzmann equation and represent the starting equation for all theoretical analyses of electron swarms in gases to the present. In conventional analyses of swarm experiments (Gibson 1970, Huxley and Crompton 1974) certain approximations and assumptions are implemented to solve this system of equations. In what follows, we highlight these assumptions and approximations and demonstrate how they are avoided in the present theory and associated code. To facilitate this we briefly review the theory used in the present analysis and refer to prior analyses where appropriate.

The design and analysis of electron swarm experiments are generally made under the assumption of the existence of the *hydrodynamic regime*. This regime exists when the swarm has evolved to a stage where its subsequent space and time evolution are governed entirely by linear functionals of the electron number density $n(\boldsymbol{r},t)$ (Kumar *et al* 1980). Under these conditions, the swarm can be fully characterized by time-independent transport coefficients. A representation of equation (1) in the hydrodynamic regime is made via a series of two expansions.

(1) A sufficient representation of the space and time dependence of the phase-space distribution function in the hydrodynamic regime is the density gradient expansion (Kumar *et al* 1980):

$$\begin{aligned} f(\boldsymbol{r},\boldsymbol{c},t) &= n(\boldsymbol{r},t) f^{(0)}(\boldsymbol{c}) - \boldsymbol{f}^{(1)}(\boldsymbol{c}) \cdot \nabla n(\boldsymbol{r},t) + \cdots, \\ &= \sum_{s=0}^{\infty} \sum_{\lambda=0}^{s} \sum_{\mu=-\lambda}^{\lambda} g(s\lambda\mu;\boldsymbol{c}) G_{\mu}^{(s\lambda)} n(\boldsymbol{r},t), \end{aligned} \tag{4}$$

where $G_{\mu}^{(s\lambda)}$ is the irreducible tensor form of the gradient operator (Robson and Ness 1986). This representation enables direct connection with the continuity and diffusion equations from which the transport coefficients are defined (see equations (9e)).

(2) The angular dependence of $f(\boldsymbol{r},\boldsymbol{c},t)$ in velocity space is generally expanded in spherical harmonics as (Robson and Ness 1986)

$$g(s\lambda\mu;\boldsymbol{c}) = \sum_{\ell=0}^{\ell_{\max}} \sum_{m=-\ell}^{\ell} f(lm|s\lambda\mu;c) Y_{\ell m}(\hat{\boldsymbol{c}}) \delta_{\mu m}, \tag{5}$$

where $\hat{\boldsymbol{c}}$ represents the angles of $\boldsymbol{c}$. If we now define the quantities

$$\begin{aligned} F_\ell^{(0)}(c) &\equiv \mathrm{i}^\ell \left[\frac{2\ell+1}{4\pi}\right]^{1/2} f(\ell 0|000;\, c) \\ F_\ell^{(\mathrm{L})}(c) &\equiv \mathrm{i}^{l+1} \left[\frac{2\ell+1}{4\pi}\right]^{1/2} f(\ell 0|110;\, c) \\ F_\ell^{(\mathrm{T})}(c) &\equiv \mathrm{i}^{l+1} \left[\frac{2(2\ell+1)}{4\pi\ell(\ell+1)}\right]^{1/2} f(\ell 1|111;\, c), \end{aligned} \tag{6a}$$

then (in the absence of non-particle-conserving collisional processes, e.g. attachment, ionization etc) the following hierarchy of equations suffices to determine the quantities of interest in the present work (Kumar *et al* 1980):

$$\begin{aligned} &\frac{l}{2l-1}\left(\frac{eE}{m}\right)\left[\frac{\mathrm{d}}{\mathrm{d}c} - \frac{l-1}{c}\right] F_{\ell-1}^{(0)}(c) + \frac{l+1}{2l+3}\left(\frac{eE}{m}\right)\left[\frac{\mathrm{d}}{\mathrm{d}c} + \frac{l+2}{c}\right] F_{\ell+1}^{(0)}(c) \\ &\qquad = -\,\hat{J}_\ell\, F_\ell^{(0)}(c) \end{aligned} \tag{7a}$$

$$\begin{aligned} &\frac{l}{2l-1}\left(\frac{eE}{m}\right)\left[\frac{\mathrm{d}}{\mathrm{d}c} - \frac{l-1}{c}\right] F_{\ell-1}^{(\mathrm{L})}(c) + \frac{l+1}{2l+3}\left(\frac{eE}{m}\right)\left[\frac{\mathrm{d}}{\mathrm{d}c} + \frac{l+2}{c}\right] F_{\ell+1}^{(\mathrm{L})}(c) \\ &\qquad = -\,\hat{J}_\ell\, F_\ell^{(\mathrm{L})}(c) + c\left[\frac{l}{2l-1} F_{\ell-1}^{(0)}(c) + \frac{l+1}{2l+3} F_{\ell+1}^{(0)}(c)\right] \end{aligned} \tag{7b}$$

$$\begin{aligned} &\frac{l-1}{2l-1}\left(\frac{eE}{m}\right)\left[\frac{\mathrm{d}}{\mathrm{d}c} + \frac{l-1}{c}\right] F_{\ell-1}^{(\mathrm{T})}(c) + \frac{l+2}{2l+3}\left(\frac{eE}{m}\right)\left[\frac{\mathrm{d}}{\mathrm{d}c} + \frac{l+2}{c}\right] F_{\ell+1}^{(\mathrm{T})}(c) \\ &\qquad = -\,\hat{J}_\ell\, F_\ell^{(\mathrm{T})}(c) + c\left[\frac{1}{2l-1} F_{\ell-1}^{(0)}(c) - \frac{1}{2l+3} F_{\ell+1}^{(0)}(c)\right], \end{aligned} \tag{7c}$$

where the superscripts L and T denote longitudinal and transverse. The matrix elements of the collision operator are defined as

$$\int Y_{\ell' m'}^*(\hat{\boldsymbol{c}})\, \hat{J}(f)\, Y_{\ell m}(\hat{\boldsymbol{c}})\, \mathrm{d}\hat{\boldsymbol{c}} = \left[\hat{J}_\ell^{\,(\mathrm{el})} + \sum_i \hat{J}_\ell^{\,(\mathrm{inel})}(i)\right] \delta_{ll'}\delta_{mm'}, \tag{8}$$

where the superscripts 'el' and 'inel' refer to the elastic and inelastic processes and the index i denotes the (inelastic) scattering process. Note that the operator $\hat{J}_\ell$ in equations (7) is the quantity in square brackets in equation (8). It is traditional to refer to the $\ell = 0$ and $\ell = 1$ members of the system (7*a*) as the isotropic and vector equations, respectively.

The treatment of the speed dependence in the coefficients $F_\ell^{(0)}(c)$, $F_\ell^{(\mathrm{L})}(c)$ and $F_\ell^{(\mathrm{T})}(c)$ in (7) is purely a matter of computational efficiency and accuracy and is discussed further in section 3.1.

Using the above definitions, the transport coefficients of interest in this research can be expressed as

$$W = \left(\frac{4\pi}{3}\right) \int c\, F_1^{(0)}(c) c^2\, \mathrm{d}c \tag{9a}$$

$$D_\mathrm{L} = \left(\frac{4\pi}{3}\right) \int c F_1^{(\mathrm{L})}(c) c^2\, \mathrm{d}c \tag{9b}$$

$$D_\mathrm{T} = \left(\frac{4\pi}{3}\right) \int c F_1^{(\mathrm{T})}(c) c^2\, \mathrm{d}c \tag{9c}$$

$$\varepsilon = 4\pi \int \frac{1}{2} m c^2 F_0^{(0)}(c) c^2\, \mathrm{d}c \tag{9d}$$

$$k_{i\to k} = 4\pi \int F_0^{(0)}(c) v \sigma^{(i\to k)}(v,\theta)\, \sin\theta\, \mathrm{d}\theta\, \mathrm{d}\boldsymbol{C}\, \mathrm{d}\boldsymbol{c}, \tag{9e}$$

where W is the drift velocity, D_{L} and D_{T} are respectively the components of the diffusion tensor parallel and perpendicular to the electric field, ε is the mean energy and $k_{i\rightarrow k}$ is the rate coefficient for the $i \rightarrow k$ excitation.

Understandably, many of the previous analyses of swarm experiments have utilized approximations which reduce mathematical complexity and facilitate analytic or at least simplified numerical solution of the system equations (7). To this end the two-term approximation (namely the truncation of the expansion (5) at $l_{\max} = 1$) has dominated the literature and indeed the analysis of electron-swarm experiments involving H_2 (Gibson 1970, Huxley and Crompton 1974). These studies invoked further approximations on the collision operator which enabled the reduction of the hierarchy of equations (generated through the above procedure) to a second-order differential equation (Gibson 1970). In contrast, for the present theory the infrastructure developed for the Boltzmann equation and the above form of the collision operator (2) in the Sonine polynomial basis (see section 3.1) is extensive and quite general in its applicability. Beyond the assumptions of the semiclassical picture and the existence of a hydrodynamic regime, *no approximations are made*. In contrast to conventional theories, we note the following for the present theory and associated code.

(1) *No assumptions are made on the number of spherical harmonics in the expansion (5).*

In the present theory this value is incremented until a specified accuracy condition is satisfied. In contrast, conventional theories typically consider only the first two terms. The inadequacy of the two-term approximation has been well documented for molecular gases (Lin *et al* 1979, Reid 1979, Ness and Robson 1986).

(2) *No assumptions are made on the action of the various collision process operators in the various spherical harmonic equations.*

In conventional theories, $\hat{J}_0^{(\mathrm{el})}$ and $\hat{J}_0^{(\mathrm{inel})}$ are reduced to (in the appropriate limits of the electron to neutral molecule mass ratio), and replaced by, the Davydov (1935) and the Frost–Phelps differential-finite-difference (Frost and Phelps 1962) collision operators respectively. In addition, in the vector equation ($l = 1$) of conventional theories, all collision processes are lumped into a single entity. In the present theory, all collision processes for all l-equations in equations (7) are treated as distinct processes.

(3) *Mass ratio effects for all collision process operators, and all order matrix elements of them, are treated in a consistent manner.*

In the present theory, the electron to neutral-molecule mass ratio dependence of $\hat{J}_l$ for all processes is represented through the expansion

$$\hat{J}_l = \sum_{p=0}^{p_{\max}} \left(\frac{m}{m+M} \right)^p \hat{J}_l(p). \tag{10}$$

In conventional theories, different levels of mass ratio approximation are employed for the various $\hat{J}_l$ and types of collision process. For example, in the isotropic equation ($l = 0$), $\hat{J}_0^{\mathrm{elast}}$ is considered to first order in the mass ratio (i.e. the Davydov operator). All other $\hat{J}_l$ for all other processes are truncated to zeroth order in the mass ratio (i.e. $p_{\max} = 0$ in equation (10)). In the present theory, we have the flexibility to increment the value of $p_{\max}$ until convergence in the transport properties is obtained.

(4) *There is no restriction on the angular dependence of the differential cross-section.*

In the present theory, the upper limit on the expansion (3*a*) can be incremented until convergence is obtained, though the value is coupled to the value of $l_{\max}$ in equation (5) and the

order of the mass ratio, $p_{\max}$ in equation (10) (namely $L_{\max} \leqslant l_{\max} + p_{\max}$). In contrast, in conventional theories, the angular dependence of the differential cross-section is restricted to $L_{\max} = 1$ and consequently only the total and momentum transfer cross-sections could be sampled in these theories.

(5) *No assumptions are made on the relative magnitudes of the cross-sections for the various collisional processes.*

In conventional theories, it was traditional to assume that the elastic momentum transfer cross-section appearing in the Davydov operator was equal to the total momentum transfer cross-section (Gibson 1970, Huxley and Crompton 1974). The validity of such an approximation has been shown to be questionable (Reid 1979). No such assumptions are needed nor employed in the present theory.

(6) *We do not neglect the temporal derivative of higher-order l components.*

Within the confines of the two-term approximation, it is traditional in the conventional theories to set the time derivative in the vector equation to zero. Errors resulting from this approximation manifest themselves only in the diffusion coefficients beyond the two-term limit (Brennan and Ness 1992). No such approximation is made in the present theory.

(7) *The thermal motion of the neutrals is systematically incorporated into all collision process operators and all spherical harmonic equations.*

The consideration of the thermal motion of the neutrals in conventional theories is generally restricted to the isotropic matrix elements of the elastic collision operator.

In section 4.4, we shall attempt to isolate some of these approximations used in conventional theories and estimate the magnitudes of their associated errors.

3.1. Computational considerations

3.1.1. Boltzmann equation. Solution of the hierarchy of equations generated through expansions (4), (5) requires further representation of the speed dependence of $f(\boldsymbol{r}, \boldsymbol{c}, t)$. This representation is purely a matter of computational efficiency and accuracy, and various techniques have been employed (see Robson and Ness (1986) for a review). In this work, we expand the coefficients in (5) in a basis of modified Sonine polynomials $R_{\nu\ell}(\alpha c)$ about a Maxwellian distribution (w) at a 'base temperature' T_b (Lin *et al* 1979, Ness and Robson 1986):

$$f(lm|s\lambda\mu; c) = w(c; T_b) \sum_{\nu=0}^{\infty} F(\nu\, \ell\, m|s\, \lambda\, \mu; \alpha) R_{\nu\ell}(\alpha c), \tag{11a}$$

where $\alpha^2 \equiv m/kT_b$ and the weight function $w(c; T_b)$ is

$$w(c; T_b) = \left(\frac{\alpha^2}{2\pi}\right)^{3/2} \exp\left(\frac{\alpha^2 c^2}{2}\right). \tag{11b}$$

The base temperature T_b in these equations is a parameter used to optimize convergence. This expansion defines the moments $F(\nu\, \ell\, m|s\, \lambda\, \mu; \alpha)$. The benefits of a Sonine basis derive from the extensive infrastructure available for an accurate systematic treatment of the collision operator (2). For reviews on the solution of the semiclassical Boltzmann equation using this basis set, the reader is referred to Lin *et al* (1979), Ness and Robson (1986) and references therein.

3.1.2. Monte Carlo simulation. In order to provide a definitive test of the validity and accuracy of the Boltzmann equation treatment, a statistically accurate Monte Carlo simulation is required. The simulation technique used is based on the null collision technique initially introduced to kinetic theory by Skullerud (1968). We employ the adaptations of Brennan and co-workers (Brennan 1990, White *et al* 1997), which avoid the need for repetitive interpolations through the use of predetermined 'look-up' tables. Look-up tables are used for (i) optimized null collision frequencies; (ii) collision probabilities and (iii) scattering angle probabilities for anisotropic scattering.

While many methods exist for improving the convergence of Monte Carlo statistics to the steady state result, the investigation of the space and time evolution of the swarm represents a future direction of this project. Our technique involves simulating an ensemble of electrons from a given initial distribution over a given time period—the displacement and velocity of all electrons being sampled at stipulated time intervals. The formulation of this 'ensemble technique' allows direct extension to the consideration of electron–electron interactions in swarm experiments—another future direction of the present project. The time-dependent transport properties of interest are then calculated using the traditional definitions:

$$\frac{\mathrm{d}\varepsilon}{\mathrm{d}t} = \frac{m}{2}\frac{\mathrm{d}}{\mathrm{d}t}\langle c^2\rangle \qquad \text{mean power in the swarm} \tag{12a}$$

$$W = \frac{\mathrm{d}}{\mathrm{d}t}\langle z\rangle = \langle c_z\rangle \qquad \text{drift velocity} \tag{12b}$$

$$D_\mathrm{T} = \frac{1}{4}\frac{\mathrm{d}}{\mathrm{d}t}(\langle x^2\rangle + \langle y^2\rangle) \tag{12c}$$

$$= \tfrac{1}{2}(\langle xc_x\rangle + \langle yc_y\rangle) \qquad \text{transverse diffusion coefficient} \tag{12d}$$

$$D_\mathrm{L} = \frac{1}{2}\frac{\mathrm{d}}{\mathrm{d}t}(\langle z^2\rangle - \langle z\rangle^2) \tag{12e}$$

$$= \langle zc_z\rangle - \langle z\rangle\langle c_z\rangle \qquad \text{longitudinal diffusion coefficient} \tag{12f}$$

where $\langle\ \rangle$ denotes an average over all swarm particles at a given time. The simulation is quite general and is capable of handling (i) elastic, inelastic and superelastic collisions, (ii) anisotropic scattering, (iii) non-zero neutral gas temperature and (iv) arbitrary charged-particle–neutral-particle mass ratios.

4. Results and discussion

4.1. Cross-sections and experimental parameters

In this study we focus exclusively on electron transport in *para*-H_2 at 77 K. This system is the simplest case in which drift velocities determined from swarm-derived cross-sections differ severely from those determined from beam-measured or theoretically calculated cross-sections. Until this case is resolved, consideration of other experimental parameters represents an unnecessary complication. We restrict the range of E/N to 0.1–10 Td (1 Td = 1 Townsend $= 10^{-21}$ V m^2), which restricts average swarm energies to the interval 0.01–0.6 eV. This range includes (i) the region of greatest disparity between the theoretical and experimental data and (ii) the region of greatest confidence in the swarm cross-sections.

We employ for the first time the *full* set of theoretical differential cross-sections (Morrison and Trail 1993). These differential cross-sections have been decomposed into partial cross-sections using the relation (3*a*). In contrast to previous works (Haddad and Crompton 1980), we do not assume that the angular dependence of the differential cross-section is energy independent. Illustrative examples of the energy variation of the angular dependence of the

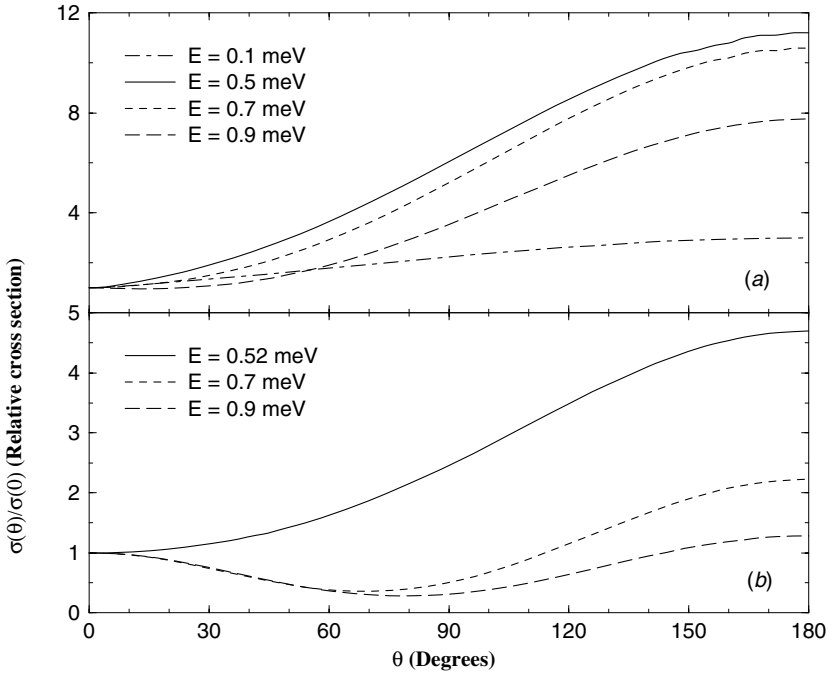

Figure 1. The angular dependence of the H_2 differential cross-sections (Morrison and Trail 1993) at selected energies for (*a*) elastic and (*b*) $v = 0 \rightarrow 1$ (pure-vibrational) processes.

differential cross-section for two collisional processes are displayed in figure 1. Furthermore in this work, ro-vibrational processes are treated explicitly, instead of being lumped into the overall vibrational cross-sections.

4.2. Foundation studies

To attempt resolution of the discrepancies between theory and experiment, we require a Boltzmann equation theory and associated code that is more accurate than both techniques from which the discrepancy originates. To this end, we have performed a series of comparative and benchmark tests to validate the present Boltzmann equation treatment. In particular, we consider those features of the molecular cross-sections which are distinct from those in the atomic case, for which there exists very good agreement between quantum mechanical and swarm-derived cross-sections. These features include large threshold energy disparities, energy variation of cross-section in the vicinity of the threshold and anisotropic scattering. We compare with an independent Monte Carlo simulation and other published results where possible. The details of the models and the results are displayed in appendix A.1. The results support the accuracy and integrity of the present theory and associated code to account for cross-sectional features distinct to molecular gases.

4.3. Direct comparison of experiment and theory

In table 1 we display the various transport coefficients calculated from the present Boltzmann equation treatment using theoretical differential cross-sections. These results are compared with the experimentally measured (Huxley and Crompton 1974) drift velocity W and ratio of the transverse diffusion coefficient to the mobility, D_T/μ. This represents the first treatment

Table 1. Comparison of theoretically determined transport coefficients using theoretical OU differential cross-sections and the present Boltzmann theory (A) with (B) experimental results (Huxley and Crompton 1974), for electrons in *para*-H_2 at 77 K.

E/n_0 (Td)		ϵ (10^{-2} eV)	W (10^3 m s^{-1})	$n_0 D_L$ (10^{23} m^{-1} s^{-1})	$n_0 D_T$ (10^{23} m^{-1} s^{-1})	D_T/μ (10^{-2} V)
0.01	A	1.0998	0.323 74	2.2159	2.4783	0.765 52
	B		0.333		2.65	0.761
0.05	A	1.7973	1.145 3	2.2263	3.1321	1.367 3
	B		1.131		3.19	1.410
0.1	A	2.3002	1.955 0	2.4404	3.4733	1.776 6
	B		1.913		3.47	1.814
0.5	A	5.5754	5.573 2	2.5180	4.7629	4.273 0
	B		5.42		4.64	4.28
1.0	A	10.145	7.366 4	2.5008	5.7816	7.848 6
	B		7.15		5.62	7.86
5	A	37.672	13.441	3.9347	8.4123	31.294
	B		13.04		8.42	32.3
10	A	56.564	19.625 0	4.6373	9.3170	47.475
	B		18.90			

using the full set of anisotropic cross-sections without further assumptions. The present Boltzmann equation treatment emphasizes the disparity between the experimental results and those obtained using the present theoretical cross-sections. Differences between the two quantities are as high as 4% over the reduced electric field range considered. Such errors are well above the quoted uncertainty for the experimental values.

Table 2 displays the excitation rates for the various collisional processes, including the relevant ro-vibrational processes. These results demonstrate why we limit our discussion to E/N values below 10 Td (or equivalently to average swarm energies less than 0.6 eV). Beyond this range, the $v = 0 \rightarrow 2$ becomes an important though unnecessary complication to our major aim.

4.4. Studies of traditional assumptions

We now turn our attention to the underlying assumptions in the conventional theory used to analyse swarm experiments and generate cross-sections. These approximations were highlighted in section 3 and the associated errors are quantified below.

4.4.1. Truncation in the l-index; two-term approximation. In tables 3 and 4 we demonstrate the convergence in the l index of the spherical harmonic expansion equation (5) of the transport coefficients. For the drift velocity, the error associated with the two-term approximation is of the order of 0.1% over the range of field strengths considered. The coefficient D_T/μ however, appears more sensitive to the value of l_{max}. The error in the two-term approximation for this quantity increases with increasing E/N; its maximum value, however, remains less than 2% and much less than the experimental uncertainty. These coefficients are calculated from averages over the entire velocity distribution and hence are primarily dependent on electrons in the bulk of the distribution. These results thus indicate that anisotropy of the velocity distribution in the bulk is relatively weak at these fields. It is interesting to note, however, that those transport properties which effectively only sample the very tail of the distribution can introduce relative errors in the two-term approximations as high as 65%, for example the

Table 2. Excitation rates for electron swarms in *para*-H_2 calculated from the Boltzmann equation solution. The rate coefficients are defined by $k_{v_0 j_0 - vj}$, where v and j denote the vibrational and rotational quantum numbers respectively. The subscript 0 refers to the initial states.

E/N (Td)	k_{elast}/N ($\times 10^{-15}$) ($m^3\ s^{-1}$)	k_{00-02}/N ($\times 10^{-16}$) ($m^3\ s^{-1}$)	k_{00-04}/N ($\times 10^{-16}$) ($m^3\ s^{-1}$)	k_{02-04}/N ($\times 10^{-16}$) ($m^3\ s^{-1}$)	k_{00-10}/N ($\times 10^{-16}$) ($m^3\ s^{-1}$)	k_{00-12}/N ($\times 10^{-16}$) ($m^3\ s^{-1}$)	k_{00-14}/N ($\times 10^{-16}$) ($m^3\ s^{-1}$)	k_{02-14}/N ($\times 10^{-16}$) ($m^3\ s^{-1}$)
0.01	4.231	1.613×10^{-3}						
0.05	5.631	8.29×10^{-3}						
0.1	6.476	3.373×10^{-2}						
0.5	10.95	5.495×10^{-1}	1.354×10^{-7}	1.689×10^{-4}				
1.0	15.95	1.411	2.553×10^{-6}	1.557×10^{-3}	5.785×10^{-7}	4.972×10^{-8}		
5.0	37.74	8.824	9.187×10^{-2}	2.546×10^{-2}	1.917×10^{-1}	1.136×10^{-1}	4.462×10^{-6}	2.328×10^{-6}
10.0	49.56	17.09	3.412×10^{-4}	5.365×10^{-2}	9.906×10^{-1}	7.802×10^{-1}	5.104×10^{-5}	2.136×10^{-3}

Table 3. Variation of the transport coefficients with l_{max} in the spherical harmonic expansion (5).

E/N (Td)	l_{max}	W ($\times 10^3$ ms^{-1})	D_T/μ (V)
0.01	1	0.3238	0.7656
	2	0.3237	0.7655
	3	0.3237	0.7655
	converged	0.3237	0.7655
0.1	1	1.955	1.780
	2	1.955	1.777
	3	1.955	1.777
	converged	1.955	1.777
1.0	1	7.371	7.920
	2	7.366	7.846
	3	7.366	7.849
	converged	7.366	7.849
10.0	1	19.64	48.12
	2	19.63	47.44
	3	19.63	47.48
	converged	19.63	47.47

Table 4. Variation of selected rate coefficients with l_{max} in the spherical harmonic expansion (5). The rate coefficients are defined by $k_{v_0 j_0 - vj}$, where v and j denote the vibrational and rotational quantum numbers respectively. The subscript 0 refers to the initial states.

E/N (Td)	l_{max}	k_{00-00}/N ($\times 10^{-15}$ m^3 s^{-1})	k_{00-02}/N ($\times 10^{-16}$ m^3 s^{-1})	k_{00-10}/N ($\times 10^{-16}$ m^3 s^{-1})	k_{00-12}/N ($\times 10^{-16}$ m^3 s^{-1})
0.1	1	6.476	0.033 73	—	—
	2	6.475	0.033 72	—	—
	3	6.476	0.033 72	—	—
	converged	6.476	0.033 72	—	—
0.5	1	10.96	55.01	4.98×10^{-14}	5.56×10^{-16}
	2	10.96	54.95	6.36×10^{-14}	7.44×10^{-16}
	3	10.96	54.95	6.39×10^{-14}	7.49×10^{-16}
	converged	10.96	54.95	6.39×10^{-14}	7.50×10^{-16}
1.0	1	15.96	1.412	5.220×10^{-7}	4.352×10^{-8}
	2	15.95	1.411	5.776×10^{-7}	4.960×10^{-8}
	3	15.95	1.411	5.785×10^{-7}	4.972×10^{-8}
	converged	15.95	1.411	5.785×10^{-7}	4.972×10^{-8}
5.0	1	37.77	8.832	0.1916	0.1134
	2	37.74	8.824	0.1917	0.1136
	3	37.74	8.824	0.1917	0.1136
	converged	37.74	8.824	0.1917	0.1136

vibrational and ro-vibrational rate coefficients at 0.5 and 1 Td. Other rate coefficients and the vibrational and ro-vibrational coefficients at higher fields sample more of the bulk electrons and the two-term approximation is an adequate representation.

It should be emphasized that the anisotropies of the velocity distribution and of the differential cross-sections are coupled. Thus it is difficult to isolate the errors associated with an inadequate representation of the velocity distribution function. In section 4.5, we isolate the influence of anisotropy in the differential cross-sections.

The results presented in this section may appear to validate the original analysis of the swarm experiments using the traditional two-term theory. One should be careful, however, in comparing the *strict* two-term approximation considered here with the traditional two-term approximation of conventional theories. The strict two-term approximation sets $l_{\max} = 1$ in equation (5), but makes none of the other assumptions of the conventional theories detailed in section 2. Further study of the additional approximations in the contemporary theory is required and is considered below.

4.4.2. Assumptions on the relative magnitudes of σ_m. An assumption in the contemporary two-term theory implies that the elastic momentum transfer cross-section appearing in the Davydov operator for elastic collisions can be replaced by the total momentum transfer cross-section. This approximation enables the reduction of the system of two coupled equations to a single second-order equation. Such an approximation would generally require that the inelastic momentum transfer cross-section be much less than the elastic component. The fact that the momentum transfer cross-section in the elastic Davydov collision operator is weighted by the electron to neutral mass ratio may relax this restriction. The validity of such an assumption however needs to be quantified and this section addresses this issue.

To investigate this approximation we replace the elastic momentum transfer cross-section

$$\sigma_m^{(\mathrm{el})}(v) = \sigma_0^{(i\to i)}(v) - \sigma_1^{(i\to i)}(v) \tag{13}$$

by the total cross-section

$$\sigma_m^{(\mathrm{total})}(v) = \sum_{ik} \frac{N_i}{N}\left[\sigma_0^{(i\to k)}(v) - \frac{v_{ik}}{v}\sigma_1^{(i\to k)}(v)\right], \tag{14}$$

where N_i is the number density of neutrals in the internal state i and N is the total neutral number density. Conservation of energy requires

$$\epsilon_i + \tfrac{1}{2}\mu v^2 = \epsilon_k + \tfrac{1}{2}\mu v_{ik}^2, \tag{15}$$

where ϵ_i denotes the internal energy of the state i and μ denotes the reduced mass of the interactive constituents. We restrict our discussion to the two-term approximation. Beyond this level of approximation a meaningful investigation of this assumption on the cross-section is diminished.

The results associated with this approximation are compared with the values in the strict two-term limit in table 5. The errors introduced by making this approximation are of the order of or less than 0.1%, surprisingly small considering the difference between the elastic and total momentum transfer cross-sections (see figure 2). The validity of this approximation for electrons in *para*-hydrogen is confirmed, but this need not be the case for all gases (Reid 1979).

4.4.3. Neglect of the recoil of the H_2-molecule in inelastic collisions. It is traditional in conventional theories to neglect the motion of the neutrals in the inelastic component of the collision operator (see e.g. the Frost–Phelps form of the inelastic collision operator used in Gibson 1970). This is equivalent to assuming an infinite mass for those neutral molecules involved in an inelastic collision. As discussed in section 3, in the present theory and associated code, the mass ratio is treated consistently over all collisional processes, though we have the flexibility to truncate any component of the collision operator at any power of the mass ratio (see equation (10)). To test the accuracy of the assumptions in the Frost–Phelps collision operator, we truncate the inelastic component of the collision operator to zeroth order in the mass ratio. The results are displayed in table 6, where they are compared with those from the

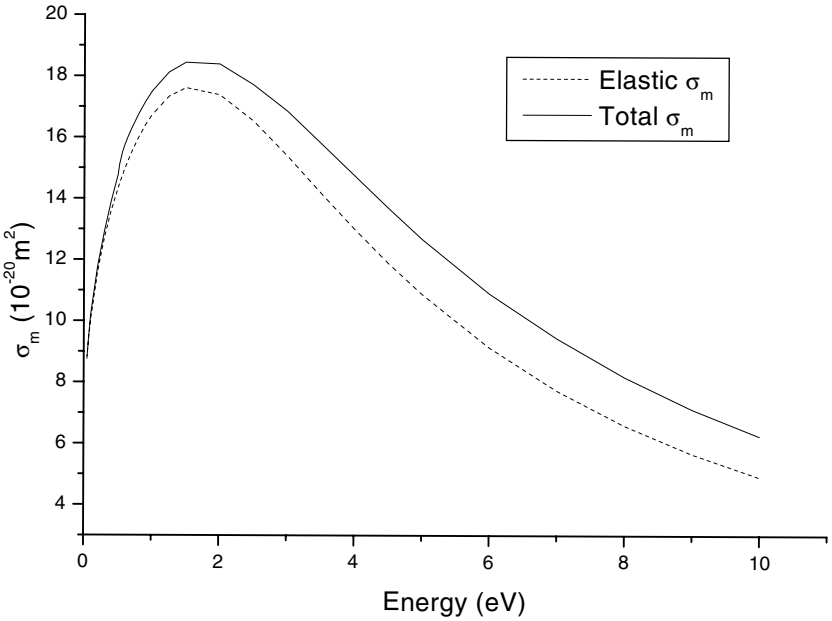

Figure 2. Comparison of the elastic momentum transfer cross-section and the total momentum transfer cross-section for e–H_2 scattering using the cross-section of Morrison and Trail (1993).

Table 5. Comparison in the two-term limit of the conventional treatment of the elastic momentum transfer cross-section (A) and the exact treatment (B).

E/n_0 (Td)		ϵ (10^{-2} eV)	W (10^3 m s^{-1})	$n_0 D_L$ (10^{23} m^{-1} s^{-1})	$n_0 D_T$ (10^{23} m^{-1} s^{-1})	D_T/μ (10^{-2} V)
0.01	A	1.0998	0.3237	2.2159	2.4783	0.765 52
	B	1.0997	0.3238	2.2160	2.4779	0.765 4
0.05	A	1.7973	1.1453	2.2263	3.1321	1.367 3
	B	1.797	1.146	2.227	3.132	1.367
0.1	A	2.3002	1.9550	2.4404	3.4733	1.776 6
	B	2.300	1.955	2.440	3.473	1.777
0.5	A	5.5754	5.5732	2.5180	4.7629	4.273 0
	B	5.576	5.573	2.517	4.763	4.273
1.0	A	10.145	7.3664	2.5008	5.7816	7.848 6
	B	10.150	7.364	2.499	5.7823	7.852
5	A	37.672	13.441	3.9347	8.4123	31.294
	B	37.71	13.43	3.937	8.414	31.32
10	A	56.564	19.625	4.6373	9.3170	47.475
	B	56.621	19.612	4.6391	9.3188	47.516

systematic treatment. The observed errors of less than 0.1% support the accuracy of the zeroth-order mass-ratio truncation of the inelastic collision operator used in conventional theories, for this gas over the range of fields considered.

4.5. Systematic investigation of anisotropic scattering

The aim of this section is to systematically investigate the influence of the anisotropic character of the theoretical differential cross-sections on the transport coefficients and other properties.

Table 6. Comparison of the zeroth-order truncation in the mass ratio for the inelastic component of the collision operator (A) and the converged multi-term results (B).

E/n_0 (Td)		ϵ (10^{-2} eV)	W (10^3 m s^{-1})	$n_0 D_L$ (10^{23} m^{-1} s^{-1})	$n_0 D_T$ (10^{23} m^{-1} s^{-1})	D_T/μ (10^{-2} V)
0.01	A	1.0998	0.3237	2.2159	2.4783	0.765 52
	B	1.0997	0.3238	2.2160	2.4779	0.765 4
0.05	A	1.7973	1.1453	2.2263	3.1321	1.367 3
	B	1.797	1.146	2.227	3.132	1.367
0.1	A	2.3002	1.9550	2.4404	3.4733	1.776 6
	B	2.300	1.955	2.440	3.473	1.777
0.5	A	5.5754	5.5732	2.5180	4.7629	4.273 0
	B	5.576	5.573	2.517	4.763	4.273
1.0	A	10.145	7.3664	2.5008	5.7816	7.848 6
	B	10.150	7.364	2.499	5.7823	7.852
5	A	37.672	13.441	3.9347	8.4123	31.294
	B	37.71	13.43	3.937	8.414	31.32
10	A	56.564	19.625	4.6373	9.3170	47.475
	B	56.621	19.612	4.6391	9.3188	47.516

Table 7. Converged multi-term transport coefficients in *para*-hydrogen at 77 K for various approximations: (A) full anisotropic cross-sections; (B) isotropic scattering only; (C) $\sigma_l = 0$ for $l > 1$ for elastic processes and $\sigma_l = 0$ for $l > 0$ for inelastic processes.

E/n_0 (Td)		ϵ (10^{-2} eV)	W (10^3 m s^{-1})	$n_0 D_L$ (10^{23} m^{-1} s^{-1})	$n_0 D_T$ (10^{23} m^{-1} s^{-1})	D_T/μ (10^{-2} V)
0.01	A	1.0998	0.323 74	2.2159	2.4783	0.765 52
	B	1.1094	0.341 62	2.3489	2.6415	0.773 22
	C	1.0998	0.323 74	2.2159	2.4783	0.765 53
0.05	A	1.7973	1.145 3	2.2263	3.1321	1.367 3
	B	1.8315	1.216 8	2.4362	3.3763	1.387 3
	C	1.7974	1.145 3	2.2264	3.1322	1.367 4
0.1	A	2.3002	1.955 0	2.4404	3.4733	1.776 6
	B	2.3392	2.095 6	2.6799	3.7578	1.793 2
	C	2.3003	1.955 1	2.4405	3.4733	1.776 6
0.5	A	5.5754	5.573 2	2.5180	4.7629	4.273 0
	B	5.8750	6.048 4	2.8924	5.3678	4.437 3
	C	5.5760	5.574 0	2.5192	4.7636	4.273 0
1.0	A	10.145	7.366 4	2.5008	5.7816	7.848 6
	B	10.986	8.095 1	3.0371	6.7607	8.351 6
	C	10.147	7.368 1	2.5026	5.7835	7.849 4
5	A	37.672	13.441	3.9347	8.4123	31.294
	B	40.859	16.011	5.3415	10.633	33.207
	C	37.683	13.447	3.9378	8.4186	31.304
10	A	56.564	19.625	4.6373	9.3170	47.475
	B	61.129	23.672	6.0603	11.982	50.616
	C	56.576	19.628	4.6342	9.3246	47.506

In previous studies, the energy and angular dependence of the differential cross-section were assumed to be separable (Haddad and Crompton 1980). In figure 1, we demonstrate the energy dependence of the differential cross-section and bring into question the validity of such an approximation. No such approximation is made here, the representation of the differential cross-section being given by equation (3*a*). Here we investigate the sensitivity of the transport coefficients and velocity distribution function to the value of $L_{\max}$ in equation (3*a*). To decouple

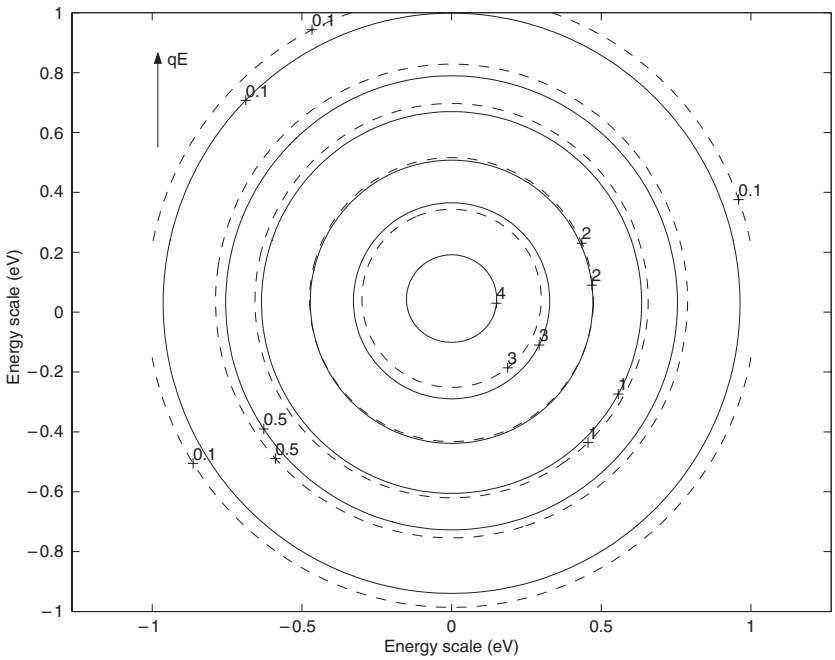

Figure 3. A comparison of the velocity distribution functions for isotropic (dashed curves) and fully anisotropic (solid curves) scattering for e–H_2 scattering using the cross-sections of Morrison and Trail (1993) ($E/N = 5$ Td). The values of the contours are $(\text{eV})^{3/2}$.

the anisotropy in the velocity distribution from that in the differential cross-section, we set $l_{\max}$ to 5. The partial cross-sections for $L > L_{\max}$ are set to zero, unless explicitly stated. The results are displayed in table 7.

The inadequacy of an isotropic scattering assumption (i.e. $L_{\max} = 0$) is emphatically demonstrated as E/N is increased. Errors of the order of 20% are observed in the measured transport coefficients. In conventional theories, truncation of equation (3*a*) at $L_{\max} = 1$ for elastic scattering and at $L_{\max} = 0$ for all inelastic processes is assumed. The application of this approximation is also displayed in table 7. The importance of this extra partial cross-section for elastic collision processes is clearly demonstrated. The errors are reduced to less than 1% in this case. The inclusion of additional partial cross-sections beyond this level of approximation (or equivalently further angular dependence in the differential cross-sections) has minimal effect on the transport coefficients.

As a further probe into the effect of anisotropic scattering, we investigate its influence on the *velocity* distribution function. The results are displayed in figure 3 for both isotropic and exact differential cross-sections in *para*-H_2. For this gas, anisotropic scattering does not manifest itself in any marked angular dependence in the velocity distribution, but rather the dominant effect appears to be in the angular integrated form—the speed/energy distribution function. The form of the velocity distribution in figure 3 supports the accuracy of the two-term approximation for electron transport in *para*-H_2 over the range of fields considered, as highlighted previously.

5. Concluding remarks

In this work, we have employed an accurate semiclassical solution of Boltzmann's equation supported by an independent Monte Carlo simulation in an attempt to resolve the disparity in

the $v = 0 \rightarrow 1$ vibrational cross-section of H_2 that has existed in the literature for many years. None of the enhancements on prior analysis accomplished this goal. We have focused on the assumptions in the traditional semiclassical theory which was used in the original analysis of the swarm experiments (Huxley and Crompton 1974); our results support the validity of this treatment.

By eliminating possible sources of error in this approach we have laid the groundwork for the next phase of this project, in which we turn to questions that reach beyond the standard model of swarm experiments. Does the conventional kinetic theory as presented here suffer from certain basic flaws? Must the fermionic nature of the electrons and electron–electron interactions be incorporated into the transport analysis? Is it meaningful to compare quantities derived from transport analysis of swarm experiments with theoretical and beam measured cross-sections? Are there heretofore unaccounted for processes operative within the drift chamber?

Acknowledgments

The authors gratefully acknowledge extremely useful conversations with Dr R K Nesbet and Professors Robert W Crompton, Malcolm Elford, Kieran Mullen and Robert Robson concerning various aspects of this research. This work was supported by the National Science Foundation under grant PHY-0071031.

Appendix. Comparative and benchmark model testing

To validate the present theory and associated code for the solution of the semiclassical Boltzmann equation, we compare against an independent Monte Carlo simulation and other theories where possible.

A.1. Model anisotropic scattering benchmarks

We employ a model introduced by Reid (1979) to investigate the influence of anisotropic scattering on electron transport. The model has served as a benchmark for multi-term solutions of Boltzmann's equation (see Ness and Robson 1986) and references therein). The details of the model under consideration are (Reid 1979)

$$\sigma_m^{\mathrm{el}} = 10\ \text{Å}^2 \text{ (elastic momentum transfer cross-section)} \tag{A.1}$$

$$\sigma_0^{\mathrm{inel}} = 0.4\,(\epsilon - 0.516)\ \text{Å}^2 \text{ (inelastic total cross-section)} \tag{A.2}$$

$$M = 2 \text{ amu},\ T_0 = 0 \text{ K}. \tag{A.3}$$

The differential cross-section is assumed separable,

$$\sigma(v, \chi) = \bar{\sigma}(v) I(\chi) \tag{A.4}$$

where the angular function I has the following forms:

$$\text{A. } I(\chi) = \text{constant} \tag{A.5}$$

$$\text{B. } I(\chi) = \cos^4 \chi \tag{A.6}$$

$$\text{C. } I(\chi) = \exp\{-1.5(1 + \cos\chi)\} \tag{A.7}$$

$$\text{D. } I(\chi) = \begin{cases} 1 & 0 \leqslant \chi \leqslant 0.134\pi \\ 0 & 0.134\,\pi \leqslant \chi \leqslant \frac{3}{4}\pi \\ 1 & \frac{3}{4}\pi \leqslant \chi \leqslant \pi. \end{cases} \tag{A.8}$$

Table A.1. Benchmark comparisons for the anisotropic scattering models of Reid (1979). (1) Present Boltzmann equation treatment; (2) present Monte Carlo treatment; (3) Monte Carlo treatment of Reid (1979); (4) Boltzmann equation treatment (Haddad *et al* 1981).

Model (Td)	Technique	ϵ (eV)	W (10^3 m s^{-1})	$n_0 D_L$ (10^{23} m^{-1} s^{-1})	$n_0 D_T$ (10^{23} m^{-1} s^{-1})	D_T/μ (10^{-2} V)
A	1	1.2293	5.2626	1.0723	1.9582	9.3025
	2	1.227	5.24	1.069	1.94	
	3	1.234	5.26		1.984	
	4		5.2560			9.308
B	1	1.2259	5.2472	1.0945	1.9046	9.0743
	2	1.227	5.26	1.10	1.90	
	3	1.229	5.24		1.898	
	4		5.2447			9.080
C	1	1.2168	5.1690	1.0337	1.8951	9.1656
	2	1.217	5.18	1.03	1.90	
	3	1.216	5.13		1.919	
	4		5.1655			9.174
D	1	1.2103	5.1399	1.0723	1.8013	8.7615
	2	1.213	5.14	1.08	1.81	
	3	1.210	5.12		1.795	
	4		5.1365			8.771

The results are contained in table A.1. They are compared with those from the independent Monte Carlo simulation, the Monte Carlo simulation of Reid and the Boltzmann equation treatment of Haddad *et al* (1981). Excellent agreement exists between all values calculated by all independent techniques, lending support to the accuracy of the present theory and its ability to accurately consider anisotropic scattering.

A.2. Threshold behaviour studies and testing

The slope of all cross-sections in the vicinity of the threshold energy can be determined theoretically *without reference to any particular scattering calculation*. It can be derived entirely from the Schrödinger scattering equation and thus is free of any physical assumptions (other than neglect of relativistic effects) or numerical precision limits. This well defined 'threshold law' stipulates how inelastic cross-sections *must* depend on energies sufficiently close to threshold. Thus, it is interesting for us to investigate the sensitivity of the transport properties to the energy variation of the cross-section near threshold. It should be emphasized, however, that *no* cross-section set that 'violates' the threshold law could possibly be correct, independent of the results from the Boltzmann equation or any other analysis.

Upto the present there have been no benchmark models which include a large separation between the threshold energies—a characteristic in the threshold energies for molecular gases. The validity of the Boltzmann equation treatment for these characteristics must be verified.

With these motivations, we implement a model with the following characteristics:

$$\sigma_0^{\mathrm{el}} = 10\ \text{Å}^2 \quad \text{(total elastic cross-section)} \tag{A.9}$$

$$\sigma_0^{\mathrm{rot}} = \begin{cases} 0.5\ \text{Å}^2 & \text{for } \epsilon > 0.044\ \text{eV (total rotational cross-section)} \\ 0 & \text{otherwise} \end{cases} \tag{A.10}$$

$$\sigma_0^{\mathrm{vib}} = \begin{cases} C\,(\epsilon - 0.516)\ \text{Å}^2 & \text{if } \epsilon < \epsilon^\star \text{ (total vibrational cross-section)} \\ 0.5\ \text{Å}^2 & \text{if } \epsilon \geqslant \epsilon^\star \end{cases} \tag{A.11}$$

$$M = 2\ \text{amu},\ T_0 = 0\ \text{K} \tag{A.12}$$

Table A.2. Transport coefficients and properties for the double-ramp model equation (A.12): (A) $C = 0.15$ Å^2 eV^{-1}; (B) $C = 0.25$ Å^2 eV^{-1}. The primed rows denote the Monte Carlo simulation results for the equivalent cases.

E/n_0 (Td)	Model / Technique	ϵ (eV)	W (10^4 m s^{-1})	$n_0 D_L$ (10^{23} m^{-1} s^{-1})	$n_0 D_T$ (10^{23} m^{-1} s^{-1})
0.5	A	0.0247	0.796	2.15	2.82
	A′	0.0249	0.793	2.16	2.84
	B	0.0247	0.796	2.15	2.82
	B′	0.0248	0.793	2.18	2.86
1.0	A	0.0415	1.25	2.24	3.44
	A′	0.0415	1.26	2.23	3.43
	B	0.0404	1.257	2.22	3.47
	B′	0.0405	1.26	2.22	3.46
5.0	A	0.3614	2.071	5.032	10.41
	A′	0.361	2.07	5.04	10.4
	B	0.3390	2.124	5.181	10.08
	B′	0.339	2.13	5.19	10.1
10.0	A	0.7193	2.819	7.879	14.77
	A′	0.719	2.82	7.89	14.8
	B	0.6300	2.990	7.724	13.78
	B′	0.630	2.99	7.72	13.8
20.0	A	1.371	3.978	10.46	20.25
	A′	1.37	3.97	10.4	20.4
	B	1.166	4.302	9.753	18.49
	B′	1.17	4.31	9.78	18.5

where C is the initial slope of the vibrational cross-section and $\epsilon^\star$ is the value of ϵ where $C(\epsilon - 0.516) = 0.5$. All scattering is assumed isotropic.

Immediately it is evident from table A.2 that the transport coefficients are particularly sensitive to the energy variation of the cross-section around threshold. The variations of the transport coefficients themselves between the two values of C are to be expected. The decreasing mean energy results from an increased loss of energy through the vibrational channel, while the increase in the drift velocity results from the reduction in the momentum transfer collision frequency associated with a reduction in the mean energy of the swarm. For mean energies in the vicinity of and greater than the threshold, the variations of the measurable transport coefficients are generally greater than 5%. This is much greater than the quoted uncertainties in the experimental measurements. Thus one would expect the violation of the threshold laws to be adequately measurable.

The agreement between Boltzmann and Monte Carlo simulation results serves again to support the accuracy and integrity of the present solution of the semiclassical Boltzmann equation.

References

Boltzmann L 1872 *Wein. Ber.* **66** 275
Brennan M J 1990 *IEEE Trans. Plasma Sci.* **19** 256
Brennan M J and Ness K F 1992 *Nuovo Cimento* D **140** 933
Buckman S J, Brunger M J, Newman D S, Snitchler G, Alston S, Norcross D W, Morrison M A, Saha B C, Danby G and Trail W K 1990 *Phys. Rev. Lett.* **65** 3253–6
Crompton R W, Gibson D K and McIntosh A I 1969 *Aust. J. Phys.* **22** 715
Crompton R W, Gibson D K and Robertson A G 1970 *Phys. Rev.* A **2** 1386

Crompton R W and Morrison M A 1993 *Aust. J. Phys.* **46** 203–29
Davydov B I 1935 *Phys. Z. Sowj. Un.* **8** 59
Ehrhardt H, Langhans L, Linder F and Taylor H S 1968 *Phys. Rev.* **173** 222
England J P, Elford M T and Crompton R W 1988 *Aust. J. Phys.* **41** 573
Frost L S and Phelps A V 1962 *Phys. Rev.* **127** 1621
Gibson D K 1970 *Aust. J. Phys.* **23** 683
Haddad G N and Crompton R W 1980 *Aust. J. Phys.* **29** 975
Haddad G N, Lin S L and Robson R E 1981 *Aust. J. Phys.* **34** 243–9
Huxley L G H and Crompton R W 1974 *The Drift and Diffusion of Electrons in Gases* (New York: Wiley)
Kumar K, Skullerud H R and Robson R E 1980 *Aust. J. Phys.* **86** 845
Lin S L, Robson R E and Mason E A 1979 *J. Chem. Phys.* **71** 3483
Linder F and Schmidt H 1971 *Z. Naturforsch.* **26a** 1603
Morrison M A, Crompton R W, Saha B C and Petrovic Z L 1987 *Aust. J. Phys.* **40** 239–81
Morrison M A and Trail W K 1993 *Phys. Rev.* A **48** 2874
Nesbet R K 1979 *Phys. Rev.* A **20** 58
Ness K F and Robson R E 1986 *Phys. Rev.* A **34** 2185
Reid I D 1979 *Aust. J. Phys.* **32** 231
Robson R E and Ness K F 1986 *Phys. Rev.* A **33** 2068.
Skullerud H R 1968 *J. Phys. D: Appl. Phys.* **1** 1567
Sun W, Morrison M A, Isaacs W A, Trail W K, Alle D T, Gulley R J, Brennan M J and Buckman S J 1995 *Phys. Rev.* A **52** 1229
Wang-Chang C S, Uhlenbeck G E and DeBoer J 1964 *Studies in Statistical Mechanics* vol 2 (New York: Wiley)
White R D, Brennan M J and Ness K F 1997 *J. Phys. D: Appl. Phys.* **30** 810